Inorganic Chemistry

ARTICLE

pubs.acs.org/IC

Microwave versus Traditional Solvothermal Synthesis of Ni_7^{II} Discs: Effect of Ligand on Exchange Reaction in Solution Studied by Electrospray Ionization-Mass Spectroscopy and Magnetic Properties

Lian-Qiang Wei,[†,‡] Kun Zhang,[†] Ying-Chun Feng,[‡] Yun-Hong Wang,[†] Ming-Hua Zeng,*[,†,‡] and Mohamedally Kurmoo*[,§]

[†]Key Laboratory of Synthetic and Natural Functional Molecule Chemistry of the Ministry of Education, Northwest University, Xi'an, 710069, People's Republic of China

[‡]School of Chemistry and Chemical Engineering, GuangXi Normal University, Guilin 541004, People's Republic of China

[§]Laboratoire DECOMET, Institut de Chimie de Strasbourg, CNRS-UMR 7177, Université de Strasbourg, 4 rue Blaise Pascal, CS 90032, 67081 Strasbourg Cedex, France

Supporting Information

ABSTRACT: A comparative evaluation of the solvothermal method of synthesis of magnetic Ni_7 discs with four different ligands using the same concentrations of reagents and temperature found microwave heating is more effective than the traditional oven one. Where the former only needs minutes, the latter needs days with an equivalence of 10 min microwave to 1 day of traditional. The size of crystals has a narrow distribution and increases with time for the microwave but is a rather wide distribution for the traditional one. Furthermore the shape of the crystals is more regular for the microwave. The four Ni_7^{II} discs of formulas $[Ni_7L_6(\mu_3\text{-}OMe)_6](ClO_4)_2$ (**1**−**3**) and $\{[Ni_7(L_4)_6(\mu_3\text{-}OMe)_6][Ni(L_4)_2]\}(ClO_4)_2$ (**4**) were synthesized as green hexagonal rods from $Ni(ClO_4)_2\cdot 6H_2O$ in mixed MeOH/MeCN solution and salicylalde Schiff base ligands (L_1 = 2-methoxy-6-(iminomethyl)phenol, L_2 = 2-ethoxy-6-(iminomethyl)phenol, L_3 = 2-methoxy-6-((methylimino)methyl)phenol, L_4 = 2-ethoxy-6-((methylimino)methyl)-phenol). X-ray structural analyses show six symmetrically positioned Ni(2) around a central Ni(1) bridged by the μ_3-methoxide and surrounded by the ligand L which also isolates the discs from one another. The perchlorate sits in the interstices, and the planar $[Ni(L_4)_2]$ of **4** also inserts itself between the discs. The structures of **1**−**3** can be regarded as ordered discotic liquid crystals. Electrospray ionization mass spectrometry of solutions showed an exchange of methoxide for hydroxide and a different distribution of $[Ni_7]$ phase with mixed (MeO/OH) core bridges, confirming a probable "step by step" substitution of MeO^- by OH^-. Magnetic studies indicate ferromagnetic interaction between Ni(1) and Ni(2) and possible antiferromagnetic between Ni(2) and Ni(2), resulting in a noncollinear system which only reaches half of the moment in 50 kOe at 2 K.

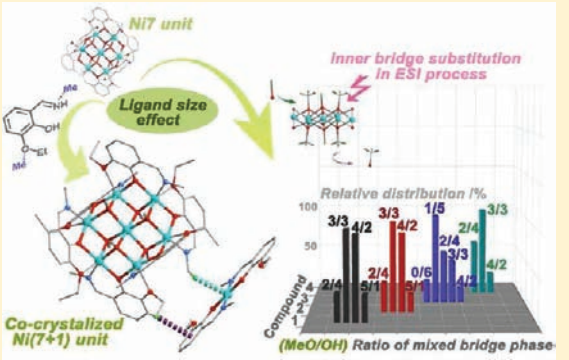

1. INTRODUCTION

Much attention has been paid to the design and the synthesis of magnetic polymetallic clusters during the past decade.[1,2] So far, multifarious magnetic clusters, including cage-like,[3] cyclic,[4] disk-like,[5] and other forms,[6] have been obtained. Among them, one important type is disk-like $[M_7]$ clusters, such as $[Mn_7]$,[7] $[Fe_7]$,[8] $[Co_7]$,[5] and $[Ni_7]$[9] complexes, have been constructed in solution by the careful selection of a "key" ligand, which dictates not only the symmetry and the topology but also the intermolecular interactions between the clusters.[10] Indeed, coordinative processes that take place in solution always accompany with great complication, which hampers the designable synthesis of such compounds, however, at the same time gives unprecedented scope to explore the principle of the coordinative reaction in the solution state. In the field of cluster-based coordination systems, great progress has been made in unraveling the formation/growth mechanism of polyoxometalate (POM)[11] and 3d metal clusters by employing electrospray ionization/cold-spray ionization mass spectrometry (ESI/CSI-Mass) spectroscopy as a tool in detecting the coordinative intermediate phases,[12] providing information about the crystal and solution states of the clusters[13] and even behaving as a technique in tracing the self-assembly process of supermolecular metal organic frameworks in solution.[14] Overall, it opens up a new avenue for the direct observation and even the controllable assembly of complex inorganic architectures.[15]

Our own interest in this area has led us to investigate the coordination chemistry of the *o*-vanillin Schiff-base ligand and its

Received: April 26, 2011
Published: June 29, 2011

dx.doi.org/10.1021/ic200883b | *Inorg. Chem.* 2011, 50, 7274–7283

Table 1. Crystal Data and Structure Refinement for 1−4[a]

complex	1	2	3	4
formula	$C_{54}H_{60}Cl_2N_6Ni_7O_{26}$	$C_{60}H_{78}Cl_2N_6Ni_7O_{26}$	$C_{60}H_{78}Cl_2N_6Ni_7O_{26}$	$C_{86}H_{114}Cl_2N_8Ni_8O_{30}$
formula weight	1690.95	1781.15	1781.15	2280.43
temperature/K	293 (2)	293 (2)	293 (2)	93 (2)
crystal system	trigonal	trigonal	trigonal	triclinic
space group	*P*-3	*P*-3	*P*-3c1	*P*-1
a/Å	14.043(2)	14.585(2)	13.936(2)	10.7335(8)
b/Å	14.043(2)	14.585(2)	13.936(2)	14.747(1)
c/Å	9.478(2)	9.621(2)	24.010(5)	16.783(1)
α/°	90	90	90	67.921(1)
β/°	90	90	90	78.637(1)
γ/°	120	120	120	89.784(1)
V/Å^3	1618.7(8)	1772.5(9)	4038.3(8)	2406.3(3)
Z	1	1	2	1
D_c/g cm^{-3}	1.741	1.669	1.465	1.574
μ/mm^{-1}	2.160	1.977	1.736	1.667
F(000)	870.0	918.0	1836.0	1184.0
no. of rflns	1907	2111	3289	8516
no. of indep rflns	1144	1062	1993	7513
R_{int}	0.0475	0.0945	0.0489	0.0179
GOF	1.107	1.069	1.137	1.077
R_1 ($I > 2\sigma(I)$)	0.0627	0.0618	0.0697	0.0528
wR_2 (all data)	0.2237	0.2356	0.2157	0.1748

[a] $R_1 = \Sigma||F_o| - |F_c||/\Sigma|F_o|$, and $wR_2 = [\Sigma w(F_o^2 - F_c^2)^2/\Sigma w(F_o^2)^2]^{1/2}$.

derivatives.[2c,10,16] Recently, our work on three ferromagnetic disk-[Co_7] compounds, [$Co_7(\mu_3\text{-}X)_6(L)_6$]·2ClO4 (X = OH^-(1), MeO^-(2), and N_3^-(3), L = methoxy-6-[(methylimino)-methyl]phenol), suggests that these compounds can be formed quickly under microwave irradiation, and the inner bridge of μ_3-MeO^- and N_3^- was found to be replaced by OH^- during the ESI-MS process, showing the different affinities of Co^{II} toward the short-bridge ligand (μ_3-OH^-, MeO^-, and N_3^-).[2c] Bearing in mind that the ligand size and corresponding Coulombic inter-ligand repulsions have a deep impression on the formation of the cluster[17] and on the similar coordination chemistry between Ni^{II} and Co^{II}, we extend our work to the microwave-assisted solvothermal synthesis of a set of disk-[Ni_7] clusters where the "key" ligand variation is initiated from 2-(iminomethyl)-6-methoxyphenol and is further functionalized by a substitutional group of different size, which results in the structural evolution from the classical [Ni_7] unit to a cocrystallization of [Ni_7] unit with a mononuclear Ni^{II} compound. At the same time, we focus on the different substitution behaviors of the core μ_3-MeO^- bridges in such clusters with similar [Ni_7] units in the ESI-MS measurements. The magnetic measurements for all the compounds are also performed.

EXPERIMENTAL SECTION

Materials and Physical Measurements. The reagents and solvents were commercially available and used as received without further purification. C, H, and N microanalyses were carried out using an Elementar Vario-EL CHNS elemental analyzer. FT-IR spectra were recorded (KBr pellets) in the range of 4000−400 cm^{-1} on a Bio-Rad FTS-7 spectrometer. Thermogravimetric (TG) analysis was performed on a Pyris Diamond TG/DTA. The ESI mass spectra were acquired using a HCT mass spectrometer (Bruker Daltonics, Germany). Temperature- and field-dependent magnetic measurements were carried out on a SQUID-MPMS-XL-5 magnetometer. Diamagnetic corrections were made using Pascal's constants.

*Synthesis. [$Ni_7(L_1)_6(OMe)_6$]·2ClO_4 (**1**).* A solution of L_1 (0.165 g, 1 mmol) in acetonitrile (4 mL) was added to a methanol solution (4 mL) of $Ni(ClO_4)_2\cdot 6H_2O$ (0.360 g, 1 mmol). The mixture was stirred for 15 min, and then 0.6 mL triethylamine was added. The mixture was placed in a 15 mL Teflon-lined autoclave and heated at 140 °C for 1−4 days. The autoclave was cooled over a period of 8 h at a rate of 10 °C h^{-1}, and green crystals were collected by filtration, washed with methanol, and dried in air. Phase pure crystals of **1** were obtained by manual separation. Yield: ca. 19.35, 33.1, 47.2, and 49.01% for 1−4 days, respectively (based on Ni). Anal. calcd. for $C_{54}H_{60}Cl_2N_6Ni_7O_{26}$: C, 40.42; H, 4.41; N, 4.71%. Found: C, 40.44; H, 4.53; N, 4.68%. IR (cm^{-1}): 3433(s), 3300(m), 2914(s), 1621(s), 1464(s), 1327(m), 1261(s), 1089(s), 885(w), 834(w), 742(m), 622(w), 586(w). **1** can also be synthesized by microwave irradiation (T = 140 °C; power = 300 W; pressure = 7.8 atm) from the same mixture at different times of 10, 20, 30, 40, and 50 min, with respective yields of 5.8, 12.64, 16.34, 24.52, and 32.60%.

*[$Ni_7(L_2)_6(OMe)_6$]·2ClO_4 (**2**).* The synthesis of **2** was similar to **1** except that L_1 was replaced by L_2 (0.151 g, 1 mmol). Yield: ca. 19.4, 19.76, 21.58, and 25.37% for 1−4 days (based on Ni). Anal. calcd. for $C_{60}H_{78}Cl_2N_6Ni_7O_{26}$: C, 40.42; H, 4.41; N, 4.71%. Found: C, 40.54; H, 4.50; N, 4.63%. IR (cm^{-1}): 3430(m), 3302(m), 2937(w), 1619(s), 1469(s), 1332(m), 1215(s), 1091(s), 987(w), 898(m), 742(m), 606(w), 507(w), 478(w). Microwave method for 10, 20, 30, 40, and 50 min yielded 5.1, 8.27, 10.81, 15.06, and 19.62%, respectively.

*[$Ni_7(L_3)_6(OMe)_6$]·2ClO_4·2MeCN (**3**).* The synthesis of **3** was similar with **1** except that L_1 was replaced by L_3 (0.165 g, 1 mmol). Yield: ca. 2.0, 4.34, 14.35, 20.47% for 1−4 days (based on Ni). Anal. calcd. for $C_{64}H_{84}Cl_2N_8Ni_7O_{26}$: C, 41.26%; H, 4.54%; N, 6.01%. Found: C, 41.11; H, 4.65; N, 6.21%. IR (cm^{-1}): 3435(m), 2934(m), 1631(s),

dx.doi.org/10.1021/ic200883b |*Inorg. Chem.* 2011, 50, 7274–7283

Table 2. Summary of Ni_7(II) Disc Clusters

compound	Ni···Ni(Å)	μ_3-X bridges	∠Ni−O−Ni (°) (μ_3-O)	∠Ni−O−Ni (°) (μ-O)	magnetic behavior
$[Ni_7(L_1)_6(OMe)_6]\cdot 2ClO_4$ (**1**)	3.107	−OMe	96.6(3)−98.2(3)	103.1(3)	F
$[Ni_7(L_2)_6(OMe)_6]\cdot 2ClO_4$ (**2**)	3.101	−OMe	96.5(3)−98.9(3)	102.6(2)	F
$[Ni_7(L_3)_6(OMe)_6]\cdot 2ClO_4$ (**3**)	3.097	−OMe	96.4(1)−98.0(1)	102.6(1)	F
$[Ni_7(L_4)_6(OMe)_6][Ni(L_4)_2]\cdot 2ClO_4$ (**4**)	3.116	−OMe	95.3(1)−98.5(1)	103.2(1)−103.5(1)	F
$[Ni_7(L_3)_6(OH)_6]\cdot 2NO_3$[9]	3.108	−OH	96.3(2)−97.8(2)	102.9(3)	F
$[Ni_7(L_3)_6(OH)_6]\cdot 2NO_3\cdot 3CH_3NO_2$[9]	3.110	−OH	96.4(1)−98.2(1)	103.6(2)	F
$[Ni_7(L_3Br^a)_6(OH)_6]\cdot 2NO_3\cdot 3CH_3CN$[9]	3.110	−OH	96.4(19)−98.8(2)	102.3(2)−103.7(2)	F

[a] L_3Br = 4-bromo-2-methoxy-6-((methylimino)methyl)phenol, and *F* = ferromagnetic interaction.

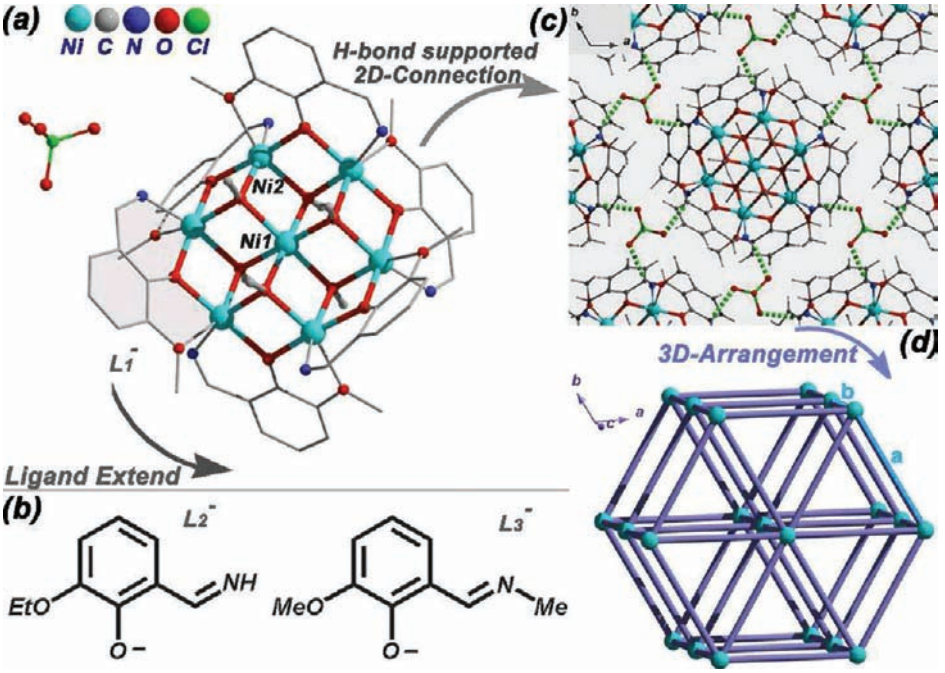

Figure 1. Compounds **1**−**3** exhibit similar structural properties: (a) the coordination environment of Ni atom in the disk-like $[Ni_7]$ unit with ClO_4^- counteranion (hydrogen atoms have been omitted for clarity); (b) ligands extend within the compound **2** and **3**; (c) crystal packing of the $[Ni_7]$ unit in the *ab* plane; (d) illustrative view of the links between clusters from one $[Ni_7]$ unit (the center···center distance in *ab* plane is represented as a and b and is the representation of that distance along the *c* direction).

1603(m), 1476(s), 1317(s), 1223(s), 1088(s), 964(m), 867(m), 746(s), 629(m), 450(w). Microwave method for 10, 20, 30, 40, and 50 min yielded 9.26, 19.54, 21.46, 25.23, and 31.84%, respectively.

*$[Ni_7(L_4)_6(OMe)_6][Ni(L_4)_2]\cdot 2ClO_4$ (**4**).* The synthesis of **4** was similar with **1** except that L_1 was replaced by L_4 (0.179 g, 1 mmol). Yield: 13.46, 24.27, 34.22, 42.7% for 1−4 days, respectively (based on Ni). Anal. calcd. for $C_{86}H_{114}Cl_2N_8Ni_8O_{30}$: C, 45.30; H, 5.04; N, 4.91%. Found: C, 45.44; H, 5.11; N, 4.98%. IR (cm^{-1}): 3667(w), 3439(m), 2931(m), 1638(s), 1550(m), 1456(s), 1322(s), 1255(m), 1229(s), 1100(s), 1012(m), 890(m), 744(s), 627(m), 484(w). Microwave method as for 10, 20, 30, 40, and 50 min yields 19.1, 24.97, 33.38, 37.84, and 42.3%, respectively.

X-ray Crystallography. The diffraction data of **1**−**4** were collected on a Bruker Smart Apex CCD diffractometer with graphite monochromated Mo−Kα radiation (λ = 0.71073 Å) at 293(2) or 93(2) K. The intensity data were corrected for Lorentz and polarization effects (SAINT), and empirical absorption corrections based on equivalent reflections were applied (SADABS).[18] All the structures were solved by direct methods and refined by the full-matrix least-squares method on F^2 with SHELXTL program package.[19] All nonhydrogen atoms were refined with anisotropic displacement parameters. Disordered segments were subjected to geometric restraints during the refinements. The hydrogen atoms of C8 in **4** were located from difference maps. The disordered guest molecules in **3** could not be modeled and were treated by the SQUEEZE routine,[20] and the guest molecules were further confirmed by TG and elemental analyses. The crystallographic details are provided in Table 1, and selected bond lengths and angles are given in Table 2. CCDC reference numbers 659672, 822901−822903. See Supporting Information for crystallographic data in CIF or other electronic formats.

RESULTS AND DISCUSSION

Crystal Structures. Crystal structures of **1**−**3**, with a formula of $[Ni_7(L)_6(\mu_3\text{-}OMe)_6](ClO_4)_2$, crystallize in trigonal space group *P*-3 for **1** and **2** and *P*-3c1 for **3**, and each consists of the cationic heptanuclear cluster (Figure 1). Disregarding the small differences in the L ligands, we find that the central cores of **1**−**3** are essentially isostructural, and their selected interatomic distances and angles are compared in Table 2. The structures of complexes

dx.doi.org/10.1021/ic200883b |*Inorg. Chem.* 2011, 50, 7274–7283

Scheme 1. Substituted Groups Extending in the Salicylalde Schiff-Base Ligands

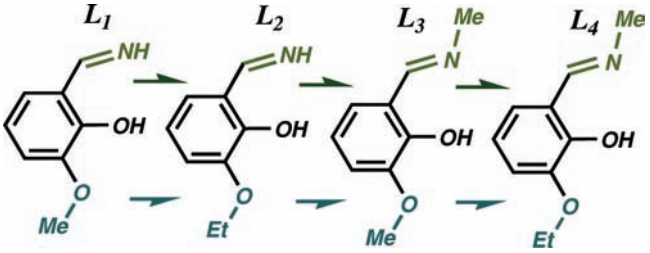

Table 3. Selected Bond Lengths [Å] and Angles [°] for 1−4

1					
Ni1—O3	2.067(6)	Ni2—O3^{i}	2.037(6)	Ni2^{i}—O1—Ni2	103.1(3)
O1—Ni2^{i}	1.978(6)	Ni2—O3	2.088(6)	Ni2^{ii}—O3—Ni1	98.2(3)
Ni2—O1	1.996(6)	Ni2—O2	2.277(7)	Ni2^{ii}—O3—Ni2	98.0(2)
N1—Ni2^{i}	2.018(9)			Ni1—O3—Ni2	96.6(3)
(i) $x-y, x, 2-z$; (ii) $y, -x+y, 2-z$					
2					
Ni1—O3	2.080(6)	Ni2—N1	2.019(7)	Ni2^{i}—O1—Ni2	102.6(2)
Ni2—O1^{ii}	1.985(6)	Ni2—O3	2.071(6)	Ni2^{ii}—O3—Ni2	98.9(3)
Ni2—O1	1.991(5)	Ni2—O2	2.330(7)	Ni2^{ii}—O3—Ni1	98.4(3)
Ni2—O3^{i}	2.013(6)			Ni2—O3—Ni1	96.5(3)
(i) $x-y, 1+x, 2-z$; (ii) $-1+y, -1-x+y, 2-z$					
3					
Ni1—O3	2.068(3)	Ni2—N1	2.062(5)	Ni2—O1—Ni2^{ii}	102.6(1)
Ni2—O1	1.977(3)	Ni2—O3^{ii}	2.079(3)	Ni2—O3—Ni1	98.0(1)
Ni2—O1^{i}	1.998(3)	Ni2—O2^{i}	2.326(4)	Ni2—O3—Ni2^{i}	98.2(1)
Ni2—O3	2.026(3)			Ni1—O3—Ni2^{i}	96.4(1)
(i) $x-y, x, 1-z$; (ii) $y, -x+y, 1-z$					
4					
Ni1—O11	2.068(3)	Ni3—N2	2.073(4)	Ni4—O1—Ni2^{i}	103.2(1)
Ni1—O10	2.070(3)	Ni3—O10	2.113(3)	Ni3—O3—Ni4	103.5(1)
Ni1—O9	2.073(3)	Ni3—O6	2.235(3)	Ni2—O5—Ni3	103.5(1)
Ni2—O5	1.984(3)	Ni4—O1	1.977(3)	Ni2—O9—Ni1	98.1(1)
Ni2—O1^{i}	2.003(3)	Ni4—O3	2.012(3)	Ni2—O9—Ni4^{i}	97.5(1)
Ni2—O9	2.046(3)	Ni4—O10	2.048(3)	Ni1—O9—Ni4^{i}	95.9(1)
Ni2—N3	2.059(4)	Ni4—N1	2.051(4)	Ni4—O10—Ni1	97.7(1)
Ni2—O11	2.109(3)	Ni4—O9^{i}	2.103(3)	Ni4—O10—Ni3	97.9(1)
Ni2—O2^{i}	2.220(3)	Ni4—O4	2.258(3)	Ni1—O10—Ni3	95.3(1)
Ni3—O3	1.986(3)	Ni5—O7	1.822(3)	Ni3—O11—Ni1	97.9(1)
Ni3—O5	2.011(3)	Ni5—N4	1.914(4)	Ni3—O11—Ni2	98.5(1)
Ni3—O11	2.032(3)			Ni1—O11—Ni2	96.3(1)
(i) $-x, -1-y, 1-z$					

1−**3** contain two counteranions ClO_4^-, a cationic cluster $[Ni_7(L)_6(\mu_3\text{-OMe})_6]^{2+}$ [L equal to ligand anion of 2-methoxy-6-(iminomethyl)phenol (L_1^-), 2-ethoxy-6-(iminomethyl)phenol (L_2^-), and 2-methoxy-6-((methylimino)methyl)phenol (L_3^-) in compounds **1**−**3**, respectively (Figure 1a and Scheme 1)], and solvent molecules in **3**. The seven Ni^{II} centers are essentially coplanar (Figure 1) as expected for all edge-sharing octahedra

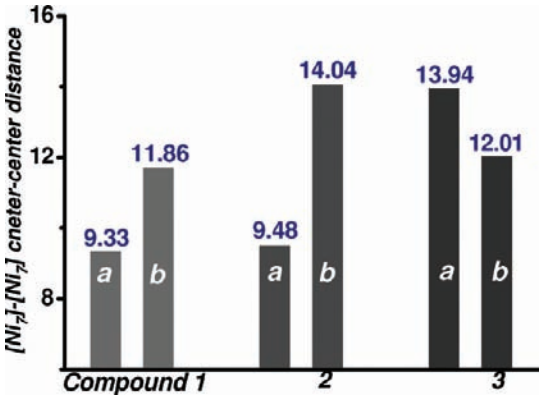

Figure 2. The crystal packing distance of the $[Ni_7]$ unit in the *ab* plane and along the *c* direction is represented as a and b, respectively.

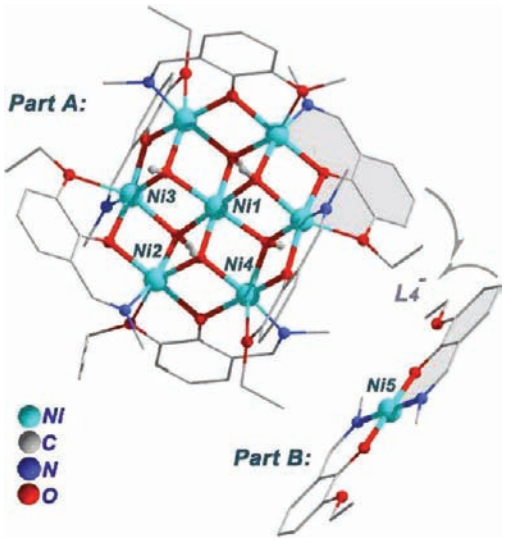

Figure 3. Molecular structures of the discrete Ni_7 cluster and mononuclear component of **4** (hydrogen atoms and ClO_4^- counteranion have been omitted for clarity).

and can be considered as a segment of the brucite $Mg(OH)_2$ layer and thus a symmetric disk. The Ni_7 units are held together by six μ_3-OMe and six O atoms of six $\eta_1{:}\eta_2{:}\eta_1{:}\mu_2$ bridging organic L ligands. The six μ_3-OMe bridge the outer Ni2 octahedra with the central Ni one with three on each surface and the six μ_2-O bridging Ni2 pairs at the periphery of the hexagon. Six N and six O atoms from the corresponding L ligand complete the peripheral ligation around the metallic core. The six L ligands are arranged as two open hemispheres with a common back and inner ligand MeO^- sitting in the bowl (Figure 1b). In **1**−**3**, the coordination bond lengths involving the μ_3-O3 atom bond lengths are in the arrangement of 2.037(6)−2.088(6), 2.013(6)−2.080(6) and 2.026(3)−2.079(3) Å, respectively (Table 3). The bridging angles of the Ni−O1−Ni bonds, which determine the sign of the magnetic exchange interactions through oxygen bridges, are 103.1(3)°, 102.6(6)°, and 102.6(1)°, respectively, and the bridging angles of the Ni−O3−Ni bonds are in the ranges of 96.6(3)−98.2(3)°, 96.5(3)−98.9(3)°, and 96.4(1)−98.0(1)°, respectively (Figure 4). The three compounds mentioned above are reminiscent of $[Ni_7(L)_6(\mu_3\text{-OH})_6](NO_3)_2$[9]

dx.doi.org/10.1021/ic200883b |*Inorg. Chem.* 2011, 50, 7274–7283

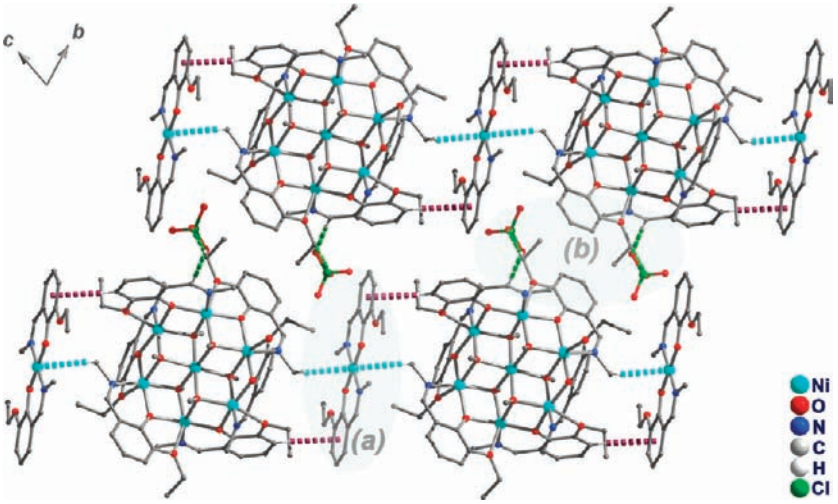

Figure 4. The crystal packing of the $[Ni_7]$ unit and the mononuclear unit in the *bc* plane of **4**. Two kinds of weak intermolecular interaction were seen: (a) the C−H···π and C−H···Ni contact between the two coordination moieties and (b) the C−H···O hydrogen bond between the ClO_4^- anion and the $[Ni_7]$ unit (hydrogen atoms have been omitted for clarity except those forming hydrogen bonds).

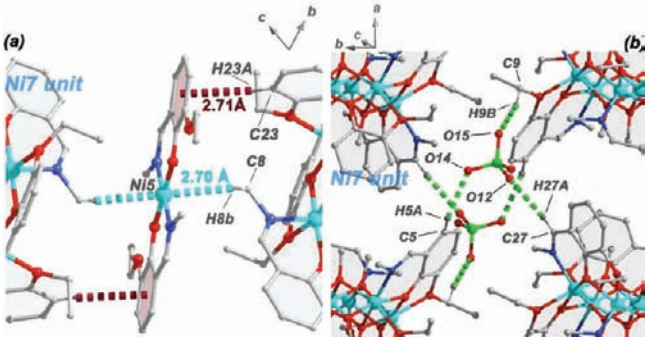

Figure 5. Detailed location of the intermolecular interaction: (a) the C−H···π and C−H···Ni contact between the two coordination moieties; (b) the C−H···O hydrogen bond between the ClO_4^- anion and the $[Ni_7]$ unit in the neighboring layer (hydrogen atoms have been omitted for clarity except those forming hydrogen bonds).

(L = 2-methoxy-6-[(methylimino)-methyl]phenol, equal to L_3 in our work), which was synthesized in the presence of NaOH, where the inner μ_3-OH^- bridged central Ni^{II} and the outer Ni^{II} octahedra with coordination bond lengths involving the μ_3-O in the range of 2.045(6)−2.088(6) Å, and the bridging angles of the Ni−(μ_3-O)−Ni were 96.3(2)−97.8(2)°, (102.9(3)° for angle of Ni−(μ_2-O) −Ni), similar values were found in **1**−**3** mentioned above. The results together with our work revealed that the Ni_7 framework can accommodate the inner μ_3-OMe being chemically replaced by OH^- without much change to the rest of the structure.

The $[Ni_7]$ units are held in 2D layers running parallel to the *ab* plane via the ClO_4^- anions, which sit above and below the individual heptanuclear complexes with N−H···O bonding interactions between the ClO_4^- and the oxygen atoms of the ligands which are absent in **3** (see Table 3 detailed hydrogen-bonding information) (Figure 1c). In this arrangement, each $[Ni_7]$ is hydrogen bonded to six ClO_4^- anions with the latter being connected to three $[Ni_7]$ units thus creating a layer with a center···center distance of 9.33, 9.48, and 13.94 Å between the

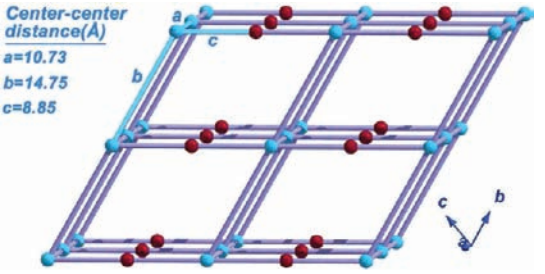

Figure 6. Illustrative view of the links between clusters of the $[Ni_7]$ unit (blue ball) and the mononuclear unit (red ball) (the center···center distance in the *bc* plane is represented as b and c, and a is the representation of the distance between the layer along *a* direction).

adjacent clusters for **1**−**3**, respectively (Figure 2), which increases in the sequence **1** < **2** < **3**, consistent with the order of ligand sizes (scheme 1). Although the ClO_4^- ions do not hold the $[Ni_7]$ moieties of neighboring layers, the layers still stack along the *c* direction forming the final 3D arrays (see Figure 1d) with a $[Ni_7]$ plane−$[Ni_7]$ plane distance of 11.68, 14.04, and 12.01 Å for **1**−**3**, respectively (Figure 2). Hence the disk-like $[Ni_7]$ units of **1**−**3** are well isolated by bulky Schiff-base ligands and ClO_4^- anions. The ligand extension seems to makes no impression on the formation of $Ni_7(\mu_3\text{-OMe})_6$ core as well as the 3D arrangement of the $[Ni_7]$ units, however, bearing in mind that the size of Schiff-base ligands extends in both the imino and the alkoxy groups, resulting in the steric hindrance that may further separate $[Ni_7]$ units in the 3D arrangement (Figure 1d).

The molecular structure of the cocrystal compound **4** contains a discrete heptanuclear cluster, $[Ni_7(L_4)_6(\mu_3\text{-OMe})_6]^{2+}$ as in **1**−**3**, a mononuclear complex, $[Ni(L_4)_2]$, and two ClO_4^- counteranions (Figure 3). The coordination properties of the $[Ni_7]$ unit in **4** share a great similarity with **1**−**3**. In the $Ni_7(\mu_3\text{-OMe})_6$ core, the coordination bond lengths involving the μ_3-O atom bond lengths are in the range of 2.070(3)−2.113(3) Å. The angles of the Ni−O−Ni bridged by μ_3-OMe are in the range of 95.9(1)−98.5(1)°, while the angles of the Ni−O−Ni bridged by μ_2-O are in the range of 103.2(1)−103.5(1)° (Table 3). Another

dx.doi.org/10.1021/ic200883b |*Inorg. Chem.* 2011, 50, 7274–7283

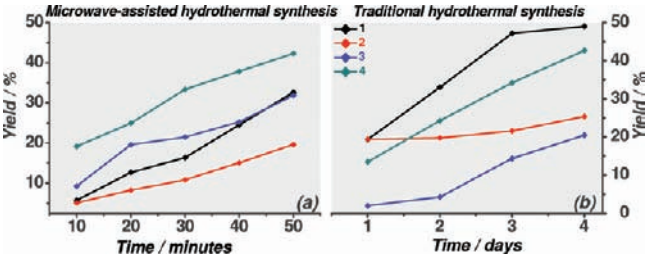

Figure 7. Comparison of the formation of compounds **1**−**4** under microwave-assisted and traditional solvothermal conditions for different periods of time.

important part comes from the mononuclear compound $[Ni(L_4)_2]$; the Ni5 ion has a N2O2 square planar coordination geometry, in which one phenolato oxygen atom and one imino nitrogen atom belonging to one deprotonated L_4^- ligand, (Ni−O: 2.019(3) Å and Ni−N: 2.059(4) Å), and the resulting mononuclear unit is thus neutral. The T-shaped C−H···π stacking interactions were observed between the $[Ni_7]$ and mononuclear units (Figures 4 and 5), which were characterized by a C−H···ring centroid contact (C23−H23a···R, R denoted as one of the aryl rings of the L_4^- ligand in the mononuclear unit) with a H···centroid distance of 2.71 Å and a ring-centroid−ring-centroid contact of 4.96 Å.[21] Another weak interunit interaction in **4** was evidenced by the short contact between Ni5 and H8b with a Ni5···H8b (C8−H8b···Ni5) bond length of 2.69(11) Å and a Ni5···C8 bond length of 3.450(6) Å, while the C8−H8b···Ni5 angle was 137.(8)°. Ni5 can be considered as a Lewis acid, where in the mononuclear unit the Ni^{II} in a square planar configuration is a 16e species with an empty orbital on the metal atom that can adapt to receive the electrons in the C−H bond. However, the contact distances of Ni5···H8b (2.69(11) Å) and Ni5···C8 (3.450(6) Å) were not comparable, and the angle was greater than 100°, thus according to G. R. Desiraju et al.,[22] the weak interaction should probably be classified as a four-electron three-center C−H···M hydrogen bond compared to those considered as agostic interactions. Thus, the mononuclear compound $[Ni(L_4)_2]$ is "locked" at the edge of the disk $[Ni_7]$ unit by C−H···π together with C−H···M hydrogen-bond interactions and stacked side by side parallel to the *bc* plane with a distance of 8.85 Å thus forming a 2D layer (Figure 6). Compared to **1**−**3**, ClO_4^- anions in **4** come into the interstices between the 2D layers and are hydrogen bonded with H12 and H30B of its neighbor (see Table S1, Supporting Information for detail information), thus connecting the 2D layers in the *a* direction and forming the final 3D arrangements with a $[Ni_7]$ plane−$[Ni_7]$ plane distance of 10.73 Å (Figure 6).

Following the observations mentioned above, the reason why the mononuclear compound only exits in **4** can be concluded as: (a) compound **1**−**3** reveals that ligand extension disperses the $[Ni_7]$ unit in 3D arrangement (Figure 2), and more substantial space would be created for accommodating guest molecules when the ligand finally reaches the size of L_4. (b) Noncovalent intermolecule interaction evolvement: the hydrogen of imino group in L_1 and L_2 functions as an ideal hydrogen bond with the ClO_4^- anion and further connects the $[Ni_7]$ unit into a 2D layer in **1** and **2**, while these kinds of hydrogen bonds are absent in **3**, distance enlargement was seen between the neighboring $[Ni_7]$ unit. When the ligand finally reaches the size of L_4, ClO_4^- anions in **4** came into the interstices and behaved as acceptors of C−H···O hydrogen bonds, while the 2D layers were accomplished by noncovalent contacts of the C−H···π and C−H···Ni hydrogen-bond interaction between the mononuclear and $[Ni_7]$ units. (c) The easy formation of the mononuclear compound with a classic square planar coordination geometry for Ni^{II} ion, which forms a coordination moiety with "just a fitting size" when coordinated to two L_4^- ligands. Indeed, the mononuclear unit was reported as early as 1990.[23] Over all, we conclude that the ligand size steric effect and the evolution of the noncovalent interaction among the $[Ni_7]$ units, the ClO_4^- anion, and the mononuclear unit directed by variation of ligand substitution together with the easy formation of the mononuclear unit controlled the structural changes from compound **1**−**4**.

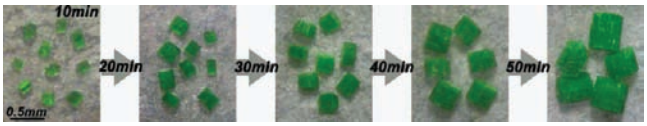

Figure 8. Series of optical microscope images of single crystals for compound **3** with different reaction times by microwave-assisted synthesis.

Microwave-Assisted Synthesis Studies. Microwave heating has proved to be a potential alternative synthetic tool in the synthesis of polymetallic complexes and may help to improve the synthetic yields.[24] Given our previous success in the microwave-assisted synthesis of a series of disk-Co_7 clusters,[2c,10a] we decided to examine whether microwave heating can be used for a similar purpose in such disk-Ni_7 clusters, which were constructed with similar salicylalde Schiff-base ligands and belonged to a samiliar structural motif.

Highly crystalline products for **1**−**4** were successfully synthesized in several minutes in a microwave field. As we suspected, a yield increase was observed for all of the compounds with the reaction time of 10−50 min (Figure 7a). In contrast, parallel experiments using traditional solvothermal synthesis in an oven needed as long as 4 days (Figure 7b) to reach the same yield. The formation process of crystal product in a microwave field was presented in Figure 8. After only 10 min, tiny green crystals with a size of ~0.15 mm were formed, most of them are suitable for single crystal X-ray analysis. Prolonging the reaction time from 10 to 40 min, the average size of crystals increases from 0.15 to 0.5 mm with good quality. Over 40 min, the products became a little coarse, and the final crystal sizes reach 0.7 mm (Figure 8). It can also be noted that the size distribution is more homogeneous and narrow for the microwave method than that of the traditional one.

The situation of microwave-assisted synthesis for **1**−**3** is consistent with the result of the disk-Co_7^{II} we reported previously,[2c] which exhibited high efficiency under microwave radiation when stabilized by salicylalde Schiff-base ligands. As was mentioned in the part of crystal structures studies, compound **4** indeed resulted from the cocrystallization of one $[Ni_7]$ unit and one mononuclear moiety. Compared to the other three compounds, significant hydrogen bonds and C−H···π stacking contacts were found between the two moieties and the ClO_4^- counteranion. From the point of molecule recognization, the time to get **4** should be longer than others. But to our surprise, the microwave-assisted synthesis time for **4** affords the most efficiency in crystal formation over **1**−**3** (Figure 7a, green line), showing the potential utilization of microwave heating in some simple coordinative systems.

dx.doi.org/10.1021/ic200883b |*Inorg. Chem.* 2011, 50, 7274–7283

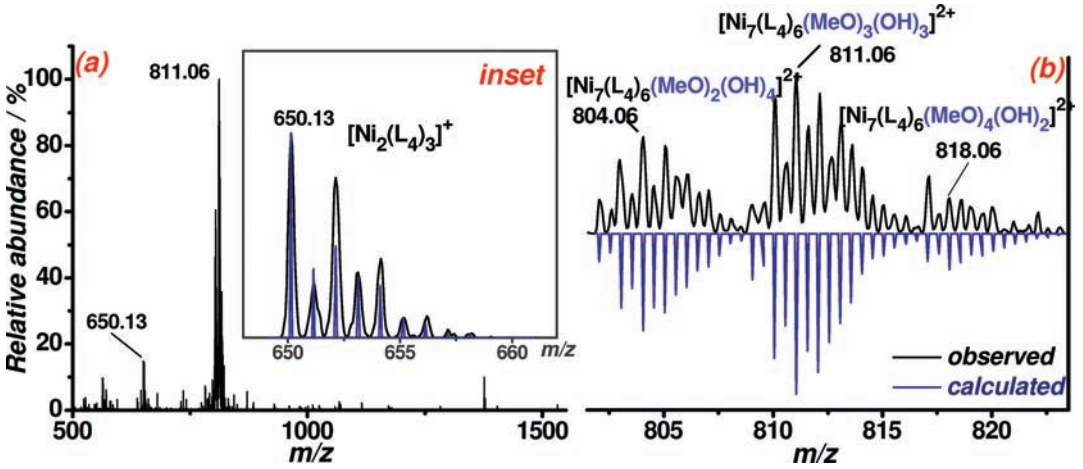

Figure 9. (a) The ESI mass spectrum of **4** in the scale of m/z = 500−1500. (b) Experimentally collected, the blue spectra are the predicted isotopic envelopes for a series of mixed CH_3O^-/OH^- core bridge compounds derived from **4**. Inset: experimentally collected and predicted isotopic envelopes for ionic peak m/z = 650.13 attributed as an ionic fragment of $[Ni_2(L_4)_3]^+$, which were arisen from the $[Ni(L_4)_2]$ mononuclear entity.

Moreover, the disk Co_7^{II} and Ni_7^{II} clusters seem to form easily under the irradiation of the microwave in our own experience. However the introduction of a microwave heating method into the hydrothermal synthesis may not always be successful when compared with a traditional one.[10a] The situation revealed that the problems associated with the system change in a coordination reaction and should be viewed from the reagents and the products for which the adsorption of microwave is different and further the formation mechanism of a cluster under the irradiation of microwave. And this will also be the future research orientation.

Inner Bridges Substitution Behavior in Solution. The ESI-MS experiments for a set of cobalt(II)-based heptanuclear clusters we reported previously have revealed a subtle substitution reaction of the core bridges (CH_3O^- and N_3^-) by OH^-, which takes place during the ESI process.[2c] In this way, we turned our attention to the behavior of the CH_3O^- inner bridges substitution in the present nickle(II)-based heptnuclear clusters.

The co-crystal compound of $[Ni_7]$ unit with a mononuclear Ni^{II}, **4**, was chosen for representation. The electrospray mass spectrum of **4** in MeCN solution is presented in Figure 9a, which exhibits a series of double charged ion peaks in the range of m/z = 801−824. Far from our speculation, there was no evidence of $[Ni_7(L_4)_6(CH_3O)_6]^{2+}$ (m/z = 833.15) cations resulting from **1** by losing two ClO_4^- anions. The ionic peak (m/z = 818.06) could be assigned to $[Ni_7(L_4)_6(MeO)_4(OH)_2]^{2+}$, indicating two core CH_3O^- bridges were replaced by a OH^- in solution. The ionic peak (m/z = 811.06) with a weight of 7 less than m/z = 818.06 can be assigned to $[Ni_7(L_4)_6(MeO)_3(OH)_3]^{2+}$, representing three core CH_3O^- bridges that were replaced by OH^-; similarly, the last isotope distribution can be assigned to $[Ni_7(L_4)_6(MeO)_2(OH)_4]^{2+}$ (m/z = 777.50) (Figure 9b). These results reveal that **4** experiences a series of ion substitutions during the ESI process,[2S] in which the core CH_3O^- bridges are replaced by OH^- sequentially. According to ESI-MS spectra, a probable "step by step" core MeO^- bridges substitution has taken place, and the "mixed−OH/MeO bridges" phase distribution with $[Ni_7(L_4)_6(MeO)_2(OH)_4]^{2+}$: $[Ni_7(L_4)_6(CH_3O)_3(OH)_3]^{2+}$: $[Ni_7(L_4)_6(CH_3O)_4(OH)_2]^{2+}$) of 2.5: 4.7: 1 based on the observed intensity. These results of the ESI-MS experiments here and those we reported earlier, where core bridge substitution of

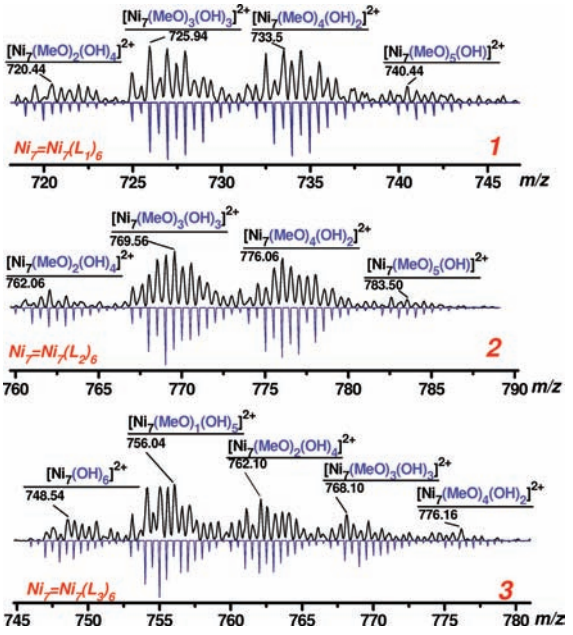

Figure 10. The ESI mass spectra of **1**−**3** experimentally collected, and the blue spectra are the predicted isotopic envelopes for a series of mixed CH_3O^-/OH^- core bridge phases.

CH_3O^-/N_3^- is replaced by OH^- for the cobalt(II) based heptanuclear clusters, suggest that the hydroxide is preferred but not totally at all six sites.[2c] Prolonged experiments will be needed to see if all can be replaced.

Another interesting issue of the ESI-MS spectra of **4** is the ionization behavior of the neutral mononuclear Ni^{II} entity. In the MS spectra of **4**, the single charged ionic peak (m/z = 650.13) with a simple isotope distribution was observed (Figure 9 inset), which can be attributed to the positive ionic phase of $[Ni_2(L_4)_3]^+$. The result prompted us to imagine that one mononuclear unit decomposition into one positive ionic phase $[Ni(L_4)]^+$ by losing one L_4^- ligand during the ESI process, and the $[Ni(L_4)]^+$ phase combines with another mononuclear unit making the detectable $[Ni_2(L_4)_3]^+$ phase (Figure S1, Supporting Information).

dx.doi.org/10.1021/ic200883b |*Inorg. Chem.* 2011, 50, 7274–7283

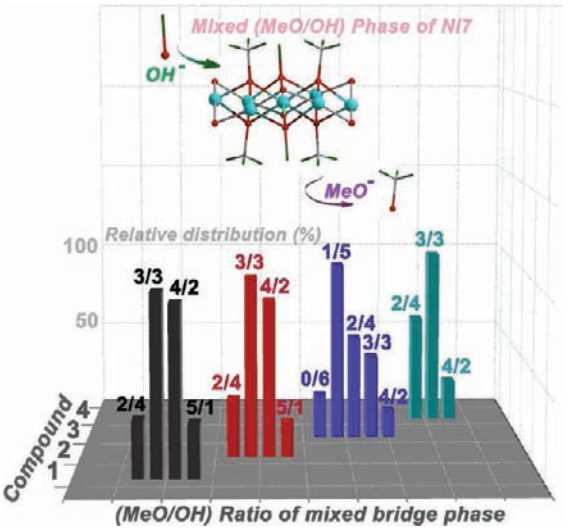

Figure 11. Summary of the relative distribution of the mixed CH_3O^-/OH^- inner bridge phase for **1**−**4**.

The electrospray mass spectrometric experiments of **1**−**3** gave the distribution "mixed-bridges" species of $[Ni_7]$ unit, as depicted in Figure 10. Nearly identical "mixed-bridges" species distributions with the MeO/OH ratio of 2/4 − 5/1 were observed for **1** and **2**, which is identical with the result we found in the disk-$[Co_7(L)_6(MeO)_6](ClO_4)_2$ [where L = 2-ethoxy-6-(iminomethyl)-phenol equal to L_2 in the present work].[10a] For **3**, a wide MeO/OH ratio of 0/6−4/2 "mixed-bridges" species distribution was observed similar to the isomorphic one constructed with cobalt(II),[2c] suggesting an easier inner bridge substitution trend compared with those of **1** and **2**. While only $[Ni_7(MeO)_2(OH)_4]^{2+}$, $[Ni_7(MeO)_3(OH)_3]^{2+}$, and $[Ni_7(MeO)_4(OH)_2]^{2+}$ (Ni_7 = $Ni_7(L_4)_6$) species were observed for compound **4**. Given the quite similar $Ni_7(\mu_3\text{-OMe})_6$ core for the four compounds, it is difficult to quantify the substitution behavior, however, based on the results we can speculate that the ability of the Schiff-base ligand in stabilizing the mixed bridge species is favored by the symmetrical ligand, as can be seen in **3**. On the other hand, the ligand extending further would result in a probable stereo hindrance at "the edge of the disc", and the substitution behavior (where the OH^- anion would attack MeO^- at "the bottom of the disc") would probably be hampered, thus making **4** standing out of the others (Figure 11).

Overall we can tentatively suggest that ESI-MS has the potential to directly probe/give mechanistic information involving the coordination reaction during the ESI process. This is because in this work we are able to observe the distribution of Ni_7 species with "mixed-bridges" in the ESI-MS experiments, while the inner-bridge substitution behavior for the four compounds differ with the ligand we used. Although the ESI-MS experiments did not reveal the full distribution of the "mixed−OH/MeO bridges" species and we cannot locate the position of MeO^- bridge that was replaced by OH^-, it is worth bearing in mind that the fast coordinative reaction of MeO^- core bridge replaced by OH^- and the stability of some $[Ni_7]$ unit with "mixed−OH/MeO bridges" might make some liable "mixed-bridges" species undetectable when conducting ESI-MS experiments. It can be imagined that this situation would be improved when ESI-MS is equipped with a cold spray or a time of flying segment.[14]

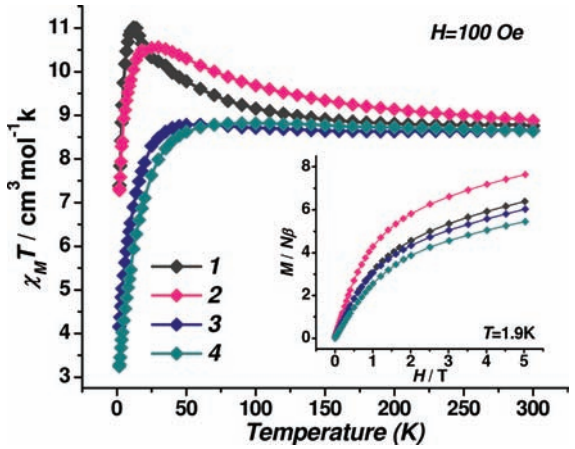

Figure 12. Temperature dependence of the magnetic susceptibility of **1**−**4** measured at 100 Oe. Inset: the field dependence of the magnetization at 2 K.

Reviewing the core bridge substition behaviors for the four compounds, we can confirm the high stability of the disk-Ni_7 framwork in MeCN solution when stabilized by the o-vanillin Schiff-base ligand[26] and the high activation of the inner MeO^- bridges by ESI-MS, thus made it a good candidate for further direct decoration from the inner bridge without the framwork being damaged, which is now on the way. In another words, with the "observation ability" of ESI-MS (and CSI-MS et al.), a route of direct structural improvment based on one as-synthesis 3d cluster with activated center would fit the strategy of controllable assembly of inorganic architectures with expected properties.

Magnetic Studies. The temperature dependence of the magnetic susceptibilities of **1**−**4** were measured on fresh polycrystalline samples with random orientation in an applied field of 100 Oe in the temperature range of 2−300 K. The magnetic moments of the four samples are almost similar (Figure 12) at room temperature with $\chi_m T$ values of 8.76, 8.87, 8.64, 8.63 $cm^3\ mol^{-1}\ K$, respectively, significantly larger than the spin-only value of seven Ni(II) ions 7.7 $cm^3\ mol^{-1}\ K$ (g = 2.1). From Figure 12, it becomes clear that there are two different "categories" of magnetic behavior for **1**−**4**; the first corresponds to **1** and **2** that displays a continuous slow increases in $\chi_m T$ upon cooling, reaching maximum values of ∼11.0 $cm^3\ mol^{-1}\ K$ at 12 K for **1** and ∼10.56 $cm^3\ mol^{-1}\ K$ at 30 K for **2**, then, decreasing upon further cooling. The low-temperature decrease is presumably due to zero-field splitting (ZFS) or intermolecular interaction. The second category is described by compounds **3** and **4** that display a value weakly increasing from 300 K with a maximum value of 8.78 $cm^3\ K\ mol^{-1}$ at 60 K for **3** and 8.81 $cm^3\ K\ mol^{-1}$ at 80 K for **4** before eventually falling to 2.0 K. The similar magnetic behavior for **3** and **4** are consistent with the structural data. Since compound **4** is a 1:1 mixture of isolated Ni_7 clusters and isolated mononuclear motifs, it is straightforward to postulate that the magnetic properties of **4** are the sum of those from Ni_7 and Ni_1, since both complexes also appear isolated. It is noted that mononuclear motif is diamagnetic, bearing testimony to the presence of square planar Ni^{II} centers, each with low-spin d^8 electron configuration. The reciprocal molar magnetic susceptibility plotted versus temperature of the four compounds obeys the Curie−Weiss law above 50 K with a C of 8.56 $cm^3\ K\ mol^{-1}$ and a θ of +6.19 K for **1**, a C of 8.37 $cm^3\ K\ mol^{-1}$ and a θ of +8.51 K for **2**, a C of 8.61 $cm^3\ K\ mol^{-1}$ and a θ of +0.91 K for **3**, and

dx.doi.org/10.1021/ic200883b |*Inorg. Chem.* 2011, 50, 7274–7283

a C of 8.61 cm^3 K mol^{-1} and a θ of +1.89 K for **4** (Figure S2, Supporting Information). The positive Weiss constants suggest that the dominant intracluster coupling is ferromagnetic, which also indicates the strength of the exchange follows the sequence **2** > **1** > **4** > **3**. The observation of ferromagnetic coupling between nickel neighbors is consistent with the previous work on disk-like structures;[9] spin frustration plays an important role, since the triangular arrangement of coupled metal ions, existing in **1**−**4**, is the textbook topology for this competing effect. Thus, the competition of ferromagnetic coupling between the central Ni^{II} (Ni1) and the peripheral ones (Ni2) and antiferromagnetic coupling between the neighboring peripheral Ni^{II} (Ni2) through μ_3-OCH_3/μ_2-oxo (L ligand) bridges within the Ni^{II} triangle is expected to lead to unusual ordering.

We investigated the variation of the magnetization M with the applied magnetic field H for **1**−**4** in the range of 0−5 T at 1.9 K (Figure 10, inset). The field dependencies of M show a rapid increase with H. The magnetization is 6.39, 7.64, 6.03, and 5.45 $N\beta$ for **1**−**4**, respectively, at 5 T, lower than the saturation values of 14 $N\beta$ for Ni_7 (assuming g = 2.00). As a means of investigating the magnetization relaxation dynamics, ac-susceptibilities of complexes **1**−**4** were studied. The ac-susceptibility measurements in a zero dc field were performed in the frequency range of 1−997 Hz. The in- and out-of-phase ac susceptibilities have no dependence on frequency between 2 and 9 K for compounds **1**−**4** (Figure S3, Supporting Information).

The magnetic data indicate that **1**−**4** have complicated magnetic structures. First, the ground states S are smaller than the sum of spin states S_T expected for ferromagnetic coupled heptanuclear Ni^{II} species, and second, the moments of the outer Ni atoms (Ni2) may be canted out of the disk plane as in an umbrella. Thus, the model we envisage is the Ni1, behaving as Ising and its moment pointing along the c-axis where as those of Ni2 behave as XY and prefer to be in the plane of the disk. Thus a compromise between the two directions is that those of Ni2 are canted along the c-axis. This picture will explain the low moment observed in the high field. The present observation is similar to that observed previously by Jones et al.,[9] which has been associated with zero-field effects.

CONCLUSION

In conclusion, we have shown how the salicylalde Schiff-base variety in ligand space can be used to mediate the 3D arrangement of the $[Ni_7]$ unit and finally a structure evolution of $[Ni_7]$ unit into a $[Ni_7][Ni_1]$ co-crystallized product of two coordination entities. The result further supports the idea that the judicious choice of "key-ligands" as building blocks may achieve a controllable assembly of the clusters. On the other hand, successful microwave-assisted synthesis for the four compounds reveals that the weak interactions (such as hydrogen bond) play an important role in accelerating the formation rate of the crystalline product and the potential utilization of microwave heating in some simple co-crystallization system. Furthermore, the successful use of electrospray mass spectrometry to probe the behavior of core bridge substitution of the $[Ni_7]$ unit reveals a probable "step by step" reaction of a MeO^- core bridge being replaced by OH^- during the ESI process, and those properties make it a good candidate for further direct decoration from the inner bridge without the $[Ni_7]$ framework being damaged, which reflects the ability of ESI-MS in making the "intermediate phase" detectable for the complex corporative reaction and thus leading a road toward a controllable cluster assembly.

Over all, with the "observation ability" of ESI-MS (and CSI-MS et al.), a route of direct structural improvement based on one as-synthesis 3d cluster with activated center would lead to a road toward a controllable cluster assembly.

ASSOCIATED CONTENT

Supporting Information. Information of weak interactions, additional structural plots, magnetism, PXRD, TGA curves, and the X-ray crystallographic files in CIF format. This material is available free of charge via the Internet at http://pubs.acs.org.

AUTHOR INFORMATION

Corresponding Author

*E-mail: zmh@mailbox.gxnu.edu.cn; kurmoo@unistra.fr.

ACKNOWLEDGMENT

This work was supported by NSFC (no. 91022015, 20871034), the Program for New Century Excellent Talents in University of the Ministry of Education China (NCET-07-217), the Project of Ten, Hundred, Thousand Distinguished Talents in New Century of Guangxi (no. 2006201), Fok Ying Tung Education Foundation (No. 111014), and the fund from CNRS-France.

REFERENCES

(1) (a) *From the Molecular to the Nanoscale: Synthesis, Structure, and Properties*; Fujita, M., Powell, A., Eds.; Creutz, C.Elsevier Ltd.: Oxford, U.K., 2004; Vol. 7. (b) Gatteschi, D.; Sessoli, R. *Angew. Chem., Int. Ed.* **2003**, *42*, 268–297.

(2) (a) Zeng, M.-H.; Yao, M.-X.; Liang, H.; Zhang, W.-X.; Chen, X.-M. *Angew. Chem., Int. Ed.* **2007**, *46*, 1832–1835. (b) Chen, Q.; Zeng, M.-H.; Zhou, Y.-L.; Zou, H.-H.; Kurmoo, M. *Chem. Mater.* **2010**, *22*, 2114–2119. (c) Zhou, Y.-L.; Zeng, M.-H.; Wei, L.-Q.; Li, B.-W.; Kurmoo, M. *Chem. Mater.* **2010**, *22*, 4295–4303.

(3) (a) Graham, A.; Meier, S.; Parsons, S.; Winpenny, R. E. P. *Chem. Commun.* **2000**, 811–812. (b) Langley, S.; Helliwell, M.; Sessoli, R.; Teat, S. J.; Winpenny, R. E. P. *Inorg. Chem.* **2008**, *47*, 497–507.

(4) (a) Brechin, E. K.; Cador, O.; Caneschi, A.; Cadiou, C.; Harris, S. G.; Parsons, S.; Vonci, M.; Winpenny, R. E. P. *Chem. Commun.* **2002**, 1860–1861. (b) Christian, P.; Rajaraman, G.; Harrison, A.; McDouall, J. J. W.; Raftery, J. T.; Winpenny, R. E. P. *Dalton Trans.* **2004**, 1511–1512.

(5) (a) Zhang, Y.-Z.; Wernsdorfer, W.; Pan, F.; Wang, Z.-M.; Gao, S. *Chem. Commun.* **2006**, 3302–3304. (b) Chibotaru, L. F.; Ungur, L.; Aronica, C.; Elmoll, H.; Pilet, G.; Luneau, D. *J. Am. Chem. Soc.* **2008**, *130*, 12445–12455. (c) Moragues-Canoás, M.; Talbot-Eeckelaers, C. E.; Catala, L.; Lloret, F.; Wernsdorfer, W.; Brechin, E. K.; Mallah, T. *Inorg. Chem.* **2006**, *45*, 7038–7040. (d) Ferguson, A.; Parkin, A.; Sanchez-Benitez, J.; Kamenev, K.; Wernsdorfer, W.; Murrie, M. *Chem. Commun.* **2007**, 3473–3475.

(6) (a) Bi, Y. F.; Wang, X.-T.; Liao, W.-P.; Zhang, H.-J.; Gao, S. *J. Am. Chem. Soc.* **2009**, *131*, 11650–11651. (b) Kong, X.-J.; Long, L.-S.; Zheng, Z.-P; Huang, R.-B.; Zheng, L.-S. *Acc. Chem. Res.* **2010**, *43*, 201–209.

(7) (a) Stamatatos, T. C.; Poole, K. M.; Fouget-Alblol, D.; Abboud, K. A.; O'Brien, T. A.; Christou, G. *Inorg. Chem.* **2008**, *47*, 6593–6595. (b) Harden, N. C.; Bolcar, M. A.; Wernsdorfer, W.; Abboud, K. A.; Streib, W. E.; Christou, G. *Inorg. Chem.* **2003**, *42*, 7067–7076. (c) Bolcar, M. A.; Aubin, S. M. J.; Folting, K.; Hendrickson, D. N.; Christou, G. *Chem.Commun.* **1997**, 1485–1486. (d) Pilawa, B.; Kelemen, M. T.; Wanka, S.; Geisselmann, A.; Barra, A. L. *Europhys. Lett.* **1998**, *43*, 7–12.

(8) (a) Oshio, H.; Hoshino, N.; Ito, T.; Nakano, M.; Renz, F.; Gütlich, P. *Angew. Chem., Int. Ed.* **2003**, *42*, 223–224. (b) Hoshino, N.; Ako, A. M.; Powell, A. K.; Oshio, H. *Inorg. Chem.* **2009**, *48*, 3396–3407.

(9) (a) Meally, S. T.; Karotsis, G.; Brechin, E. K.; Papaefstathiou, G. S.; Dunne, P. W.; McArdle, P.; Jones, L. F. *CrystEngComm* **2010**, *12*, 59–63. (b) Meally, Seán T.; McDonald, C.; Karotsis, G.; Papaefstathiou, G. S.; Brechin, E. K.; Dunne, P. W.; McArdle, P.; Power, N. P.; Jones, L. F. *Dalton Trans.* **2010**, *39*, 4809–4816.

(10) (a) Wei, L.-Q.; Li, B.-W.; Hu, S.; Zeng, M.-H. *CrystEngComm* **2011**, *13*, 510–516. (b) Li, B.-W.; Zhou, Y.-L.; Chen, Q.; Zeng, M.-H. *Polyhedron* **2010**, *29*, 148–153.

(11) Long, D.-L.; Tsunashima, R.; Cronin, L. *Angew. Chem., Int. Ed.* **2010**, *49*, 1736–1758.

(12) (a) Newton, G. N.; Cooper, G. J. T.; Kögerler, P.; Long, D.-L.; Cronin, L. *J. Am. Chem. Soc.* **2008**, *130*, 790–791. (b) Yan, J.; Long, D.-L.; Wilson, E. F.; Cronin, L. *Angew. Chem., Int. Ed.* **2009**, *48*, 4376–4380.

(13) (a) Cooper, G. J. T.; Newton, G. N.; Kögerler, P.; Long, D.-L.; Engelhardt, L.; Luban, M.; Cronin, L. *Angew. Chem., Int. Ed.* **2007**, *46*, 1340–1344. (b) Cooper, G. J. T.; Newton, G. N.; Long, D.-L.; Kögerler, P.; Rosnes, M. H.; Keller, M.; Cronin, L. *Inorg. Chem.* **2009**, *48*, 1097–1104.

(14) Chan, Y.-T.; Li, X.-P.; Soler, M.; Wang, J.-L.; Wesdemiotis, C.; Newkome, G. R. *J. Am. Chem. Soc.* **2009**, *131*, 16395–16397.

(15) (a) Miras, H. N.; Wilson, E. F.; Cronin, L. *Chem. Commun.* **2009**, 1297–1311. (b) Seeber, G.; Cooper, G. J. T.; Newton, G. N.; Rosnes, Mali, H.; Long, D.-L.; Kariuki, B. M.; Kögerler, P.; Cronin, L. *Chem. Sci.* **2010**, *1*, 62–67.

(16) (a) Zhang, S.-H.; Zhou, Y.-L.; Sun, X.-J.; Wei, L.-Q.; Zeng, M.-H.; Liang, H. *J. Solid State Chem.* **2009**, *182*, 2991–2996. (b) Zhang, S.-H.; Song, Y.; Liang, H.; Zeng, M.-H. *CrystEngComm* **2009**, *11*, 865–872.

(17) Graham, A. R.; Meier, S.; Parsons, S.; Winpenny, R. E. P. *Chem. Commun.* **2000**, 811–812.

(18) Sheldrick, G. M. *SADABS*, Program for Empirical Absorption Correction of Area Detector Data; University of Göttingen: Göttingen, Germany, 1996.

(19) Sheldrick, G. M. *SHELXL97 and SHELXTL Software Reference Manual*,version 5.1l Brucker AXSm Inc.L Madison, WI, 1997.

(20) Sheldrick, G. M. *SADABS 2.05*; University Göttingen: Göttingen, Germany, 2002.

(21) (a) Janiak, C.; Temizdemir, Savas.; Dechert, S.; Deck, W.; Girgsdies, F.; Heinze, J.; Kolm, M. J.; Scharmann, T. G.; Zipffel, O. M. *Eur. J. Inorg. Chem.* **2000**, 1229–1241. (b) Hobza, P.; Selzle, H. L.; Schlag, E. W. *Chem. Rev.* **1994**, *94*, 1767–1785.

(22) (a) Castro, M.; Cruz, J.; López-Sandovalb, H.; Barba-Behrens, N. *Chem. Commun.* **2005**, 3779–3781. (b) Thakur, T. S.; Desiraju, G. R. *Chem. Commun.* **2006**, 552–554.

(23) Kamenar, B.; Kaitner, B.; Stefanović, A.; Waters, T. N. *Acta Crystallogr., Sect. C* **1990**, *46*, 1627–1631.

(24) (a) Millos, J.; Whittaker, A. G.; Brechin, E. K. *Polyhedron* **2007**, *26*, 1927–1933. (b) Milios, C. J.; Prescimone, A.; Sanchez-Benitez, J.; Parsons, S.; Murrie, M.; Brechin, E. K. *Inorg. Chem.* **2006**, *45*, 7053–7055. (c) Milios, C. J.; Whittaker, A. G.; Fabiani, F. P. A.; Parsons, S.; Murrie, M.; Perlepes, S. P.; Brechin, E. K. *Inorg. Chem.* **2006**, *45*, 5281–5283.

(25) Pramanik, B. N.; Ganguly, A. K.; Gross, M. L. *Applied Electrospray Mass Spectrometry*; Marcel Dekker: New York, 2002; p13.

(26) Henkelis, J. J.; Jones, L. F.; De Miranda, M. P.; Kilner, C. A.; Halcrow, M. A. *Inorg. Chem.* **2010**, *49*, 11127–11132.